Highly fluorescent hybrid pigments from anthocyanin- and red wine pyroanthocyanin-analogs adsorbed on sepiolite clay

Gustavo Thalmer M. Silva, Karen M. da Silva, Cassio P. Silva, Ana Clara B. Rodrigues, Jessy Oake, Marcelo H. Gehlen, Cornelia Bohne, & Frank H. Quina

May 2019

# Highly fluorescent hybrid pigments from anthocyanin- and red wine pyranoanthocyanin-analogs adsorbed on sepiolite clay

Gustavo Thalmer M. Silva,[1] Karen M. da Silva,[2] Cassio P. Silva,[1] Ana Clara B. Rodrigues,[3] Jessy Oake,[4] Marcelo H. Gehlen,[5] Cornelia Bohne,[4] Frank H. Quina*,[1]

[1]Instituto de Química, Universidade de São Paulo, Av. Lineu Prestes 748, Cidade Universitária, São Paulo 05508-000, Brazil

[2]Instituto Federal de Educação, Ciência e Tecnologia de São Paulo, Campus São Paulo, 01109-010 São Paulo, Brazil

[3]CQC, Department of Chemistry, University of Coimbra, P3004-535 Coimbra, Portugal.

[4]Department of Chemistry and Centre for Advanced Materials and Related Technologies (CAMTEC), University of Victoria, PO Box 1700 STN CSC, Victoria, BC, Canada, V8W 2Y2

[5]Instituto de Química de São Carlos, Universidade de São Paulo, 13566-590 São Carlos, SP, Brazil

* Corresponding author.
E-mail address: quina@usp.br

## Abstract

Flavylium cations serve as models for the chemical and photochemical reactivity of anthocyanins, the natural plant pigment responsible for many of the red, blue and purple colors of fruits and flowers. Likewise, pyranoflavylium cations serve as models of the fundamental chromophoric moiety of pyranoanthocyanins, molecules that can form from reactions of grape anthocyanins in red wines during their maturation. In the present work, hybrid pigments are prepared by the adsorption of a series of five synthetic flavylium cations (FL) and five synthetic pyranoflavylium cations (PFL) on sepiolite clay (SEP). The FL are smaller in size than the PFL, but both can in principle fit into the tunnels and/or external grooves (with dimensions of 3.7 x 10.6 Å) of SEP. Measurements of the fluorescence quantum yields of the adsorbed dyes indicate that they are at least as fluorescent as in acidic acetonitrile solution, and in a few cases substantially more fluorescent. The observation of biexponential fluorescence decays is consistent with emission from dye molecules adsorbed at two distinct sites, presumably tunnels and grooves. These hybrid materials also have improved properties in terms of stability of the color in contact with pH 10 aqueous solution and resistance to thermal degradation of the dye. SEP thus appears to be a promising substrate for the development of highly fluorescent flavylium or pyranoflavylium cation-derived hybrid pigments with improved color and thermal stability.

## Graphical abstract

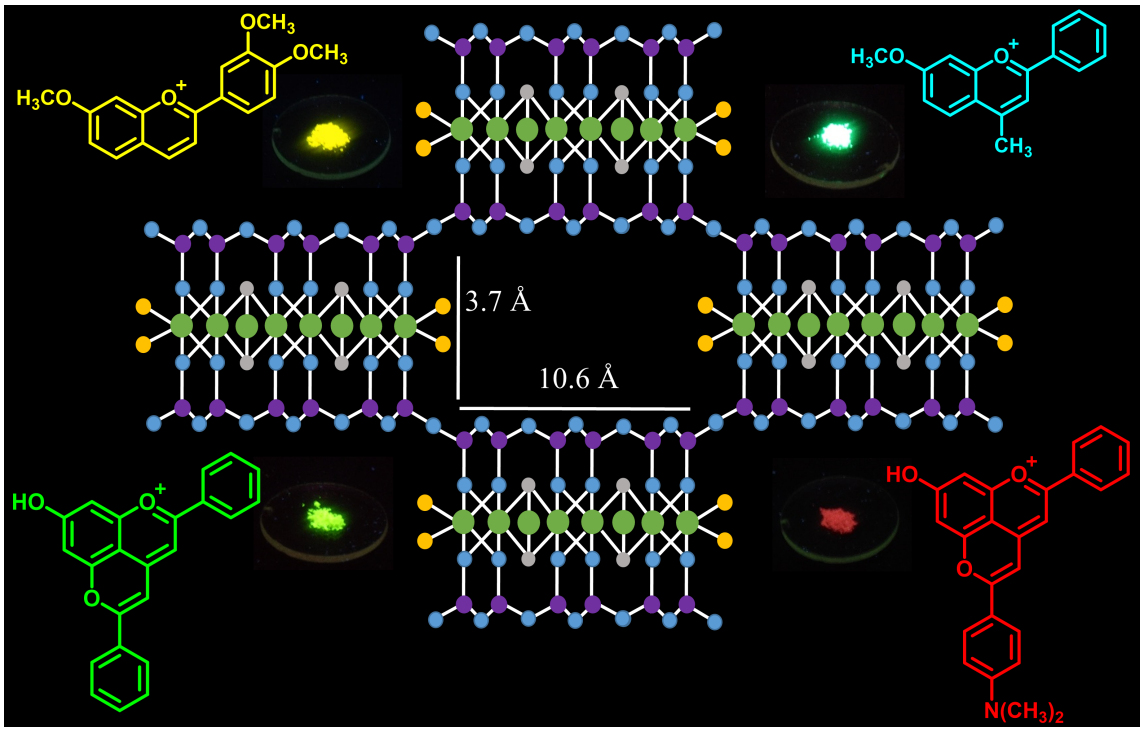


Adsorption of flavylium and pyranoflavylium cations on sepiolite clay produces highly fluorescent hybrid pigments with improved color and thermal stability.

## 1. Introduction

Sepiolite is a hydrated magnesium phyllosilicate clay mineral with fibrous morphology whose structure consists ribbons of octahedral sheets of magnesium oxides sandwiched between two tetrahedral sheets of silicon oxides with periodic inversion of the apical oxygen in every three silicate chairs. This causes a periodic discontinuity of the octahedral sheet that results in the formation of a structure with alternating blocks and one-dimensional tunnels with dimensions of 3.7 x 10.6 Å.[1,2] and, on the external surface of the clay fibers, partially open channels or grooves.[3,4] Two types of water molecules complete the tunnel structure of the sepiolite, weakly bound water in the tunnels (commonly called zeolitic water) and more tightly bound water coordinated to Mg ions at the ribbon borders (structural water molecules).[4] Its wide tunnels allows the penetration and/or adsorption of organic molecules, making SEP a good host, but its well-defined porous structure, similar to that of zeolites, does not permit lamellar expansion of SEP.[3–6]

Sepiolite was one of the clays used in the preparation of Maya Blue pigment, an ancient organic-inorganic hybrid material used in murals, codices, ceramic and sculptures by the Maya civilization in the Pre-Columbian era. Maya blue has attracted attention due to its exceptional chemical and photochemical stability, being able to withstand the attacks of acids, bases and organic solvents and exposure to light without losing its color.[7–9] The structure of Maya Blue, which is responsible for promoting this amazing stability, consists of the dye indigo protectively (and apparently irreversibly) inserted into the tunnels of palygorskite or sepiolite clay.[9–13] Many studies have focused on the characterization and stabilities of these complexes with the objective of understanding the indigo-palygorskite or indigo-sepiolite interactions in Maya Blue.[10–20] Maya Blue has also inspired the development of new materials based on the association of other dyes

with palygorskite and sepiolite, associating similar properties and enhanced stability with other colors and potential applications. These include hybrid materials with interesting self-cleaning properties[21–23] and highly stable hybrid pigments with a range of colors formed with both organic dyes[24–32] and inorganic pigments.[33–35]

Our attention was drawn to these hybrid materials as part of our interest in manipulating and controlling the chemistry of flavylium and pyranoflavylium cations. Flavylium cations are synthetic analogues containing the same fundamental chromophore as anthocyanins, the natural plant pigments responsible by the most of the blue, red and purple colors of flowers, fruits and leaves. Pyranoflavylium cations are analogs of the chromophore of pyranoanthocyanins, compounds that are formed during the maturation of red wine[36–38] via chemical reactions of grape anthocyanins with yeast metabolic products, colorless copigment molecules or other additives present in the wine.[39–44] Unlike these much more complex natural products, synthetic flavylium and pyranoflavylium cations have the advantage of relatively facile and versatile modification of the substituents and consequently the reactivity and photophysical properties of the chromophore. Having recently shown that the adsorption of flavylium cations on palygorskite resulted in hybrid pigments with greatly improved chemical and thermal stability,[45] we now report results for hybrid materials prepared by the adsorption of a series of flavylium and pyranoflavylium cations on sepiolite clay. The choice of sepiolite was dictated by the fact that its tunnels and grooves are wider than those of palygorskite and hence more attractive as a substrate for the adsorption of the larger pyranoflavylium cations.

## 2. Experimental section

### 2.1 Materials

The flavylium (FL) and pyranoflavylium (PFL) cations used in this work (Scheme 1) were available from previous studies of the group and the syntheses have been reported previously.[46–48] The sepiolite (SEP) used in this work was SepSp-1 reference clay from the Clay Minerals Society Source Clay Minerals Repository; this material was manually ground to a powder that passed freely through a 40 mesh wire sieve but otherwise used with no additional purification. The chemical composition, characterization and properties of this clay have been described.[49–56] Trifluoroacetic acid, (TFA, Sigma-Aldrich) and ethanol (Merck) were used as received.

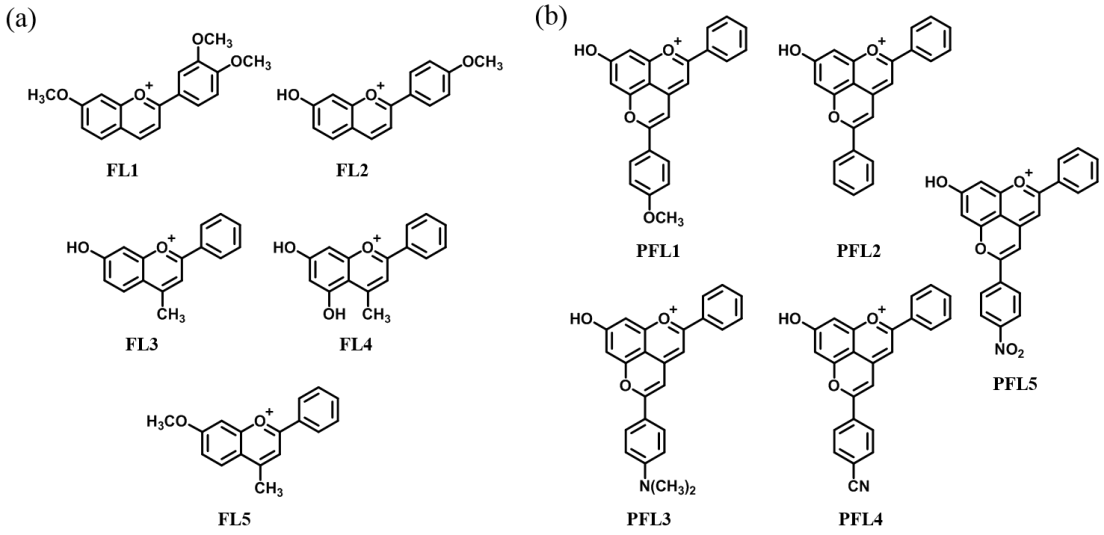


**Scheme 1.** Structures of the (a) flavylium cations, FL, and (b) pyranoflavylium cations, PFL, used in this work.

### 2.2 Preparation of the FL/SEP and PFL/SEP Hybrid Materials

Aliquots of solutions of the FL and PFL in ethanol (EtOH) acidified with 0.01 M TFA (in order to maintain the 7-OH group protonated) were added to a weighed amount

of SEP clay powder. The initial FL/SEP and PFL/SEP ratios utilized were ca. 0.03 mmol/g. The resulting suspensions were stirred for 24 h in the dark at room temperature, centrifuged and the solid washed exhaustively with TFA-acidified EtOH and then dried under vacuum for 2 h at room temperature. The amounts of FL and PFL adsorbed on SEP were estimated from the decrease in the absorbance of the supernatant employing the known molar attenuation coefficients of the FL and PFL cations.[46–48]

**2.3 UV-Vis-diffuse reflectance and fluorescence measurements.**

A Varian Cary 50 UV-Vis Bio spectrophotometer equipped with a *Barrelino*™ diffuse reflectance probe (Harrick Scientific Products, Inc.) was used for obtain UV-Vis-diffuse reflectance (DR) spectra. The corresponding CIELAB Color coordinates (CIE L*a*b*)[57] were determined with the software Agilent Cary WinUV Color employing natural daylight illuminant CIE D65 as the standard illuminant and an observer angle of 2 degrees. The remission spectra were obtained from the UV-Vis-DR employing the Kubelka-Munk equation:[58]

$$F(R) = \frac{(1-R)^2}{2R} \quad (1)$$

where R is the absolute reflectance at each wavelength.

Steady state fluorescence measurements were performed with a Hitachi F-4500 fluorescence spectrophotometer equipped with a solid sample holder. The excitation and emission wavelengths are indicated in the figure legends. The bandwidths were 2.5 nm for both excitation and emission monochromators for all measurements, except for the FL4/SEP samples (5.0 nm).

Time-resolved fluorescence decay experiments were performed as described previously.[45] The powder samples were excited at 405 nm (Edinburgh Instruments EPL

405 picosecond pulsed diode laser) in a solid sample holder and the decays collected at: 475 nm (for PFL2/SEP), 490 nm (for FL2/SEP), 500 nm (for FL3/SEP, FL4/SEP, FL5/SEP and PFL1/SEP), 515 nm (for PFL4/SEP), 525 nm (for PFL3/SEP and PFL5/SEP) or 555 nm (for FL1/SEP).

### 2.4 Confocal fluorescence microscopy

Confocal fluorescence images were obtained with the instrument and conditions described previously,[45] with the exception of the excitation wavelength and the objective. The samples were excited at 405 nm with a Coherent Cube CW laser and the polarized laser beam was focused on the samples with a 100x objective.

### 2.5 Solid state fluorescence quantum yields

The solid-state fluorescence quantum yields ($\Phi_f$) of the powder samples were measured with a Hamamatsu Quantaurus QY absolute photoluminescence quantum yield spectrometer model C11347 (integrating sphere), using raw SEP as the reference at the excitation wavelength used to obtain the spectra.

### 2.6 Sensitivity to pH and thermal stability

The reactivity of the FL and PFL cations adsorbed on SEP was investigated by addition of 15 mg of the FL1/SEP and PFL3/SEP samples to 5 mL of 10 mmol $dm^{-3}$ sodium borate buffer solution, pH = 10. The samples were stirred for 24 h, then centrifuged and dried. UV-Vis-DR spectra as well as color coordinates were obtained in order to verify any spectral or color variations. To investigate the reversibility of the adsorption, FL1 was added to 10 mmol $dm^{-3}$ sodium acetate buffer solutions at pH = 4, 5, and 6, followed by the addition of 0.05 g of SEP after discoloration of the solutions

due to the hydration of FL1. This experiment was carried out under stirring at room temperature (ca. 20 °C) and accomplished by taking digital images as a function of time.

Thermal stability was investigated by submitting FL1/SEP and PFL3/SEP samples to heating at 105 °C and 120 °C under vacuum for 24 h. Measurements of the color coordinates and UV-Vis-DR were used to verify any color or spectral changes.

## 3. Results and discussion

### 3.1 Fluorescent hybrid pigment formation

The cation exchange capacity (CEC) reported for the SepSp-1 Source Clay Sepiolite utilized in this work is 15 μmol $g^{-1}$,[56] well below the values in the range of 90-150 μmol $g^{-1}$ for SEP from Zafer Mining Co. (Balıkesir, Turkey),[59] Eskishehir Turkey[60] or Pangel-S9, Tolsa S.A..[61] Taking into account this value of the SEP cation exchange capacity, 30 μmol of FL and PFL per g of SEP (twice the CEC) were added initially in the adsorption process. Since both FL and PFL cations are highly soluble in ethanol, exhaustive washing with acidic ethanol should remove any excess or weakly physiosorbed dye, leaving only the more strongly bound dye, indicating ion exchange as potentially the most important mode of interaction of these cationic dyes with the SEP clay. Substituents on the FL or PFL cations had little or no effect on the adsorption since the final amounts of adsorbed dye were similar for all dyes after the washing step. In addition, all of the amounts of adsorbed dye were inferior to the reported cation exchange capacity (CEC) of 15 μmol $g^{-1}$ [56] for the clay, suggestive of the importance of ion exchange in the adsorption process under these conditions. Although FL cations are slightly smaller in size than PFL cations, the dimensions of both classes of dyes relative to those of the tunnels (Figure 1) should permit some insertion of the dyes into the tunnels, in addition to inclusion in the external grooves.

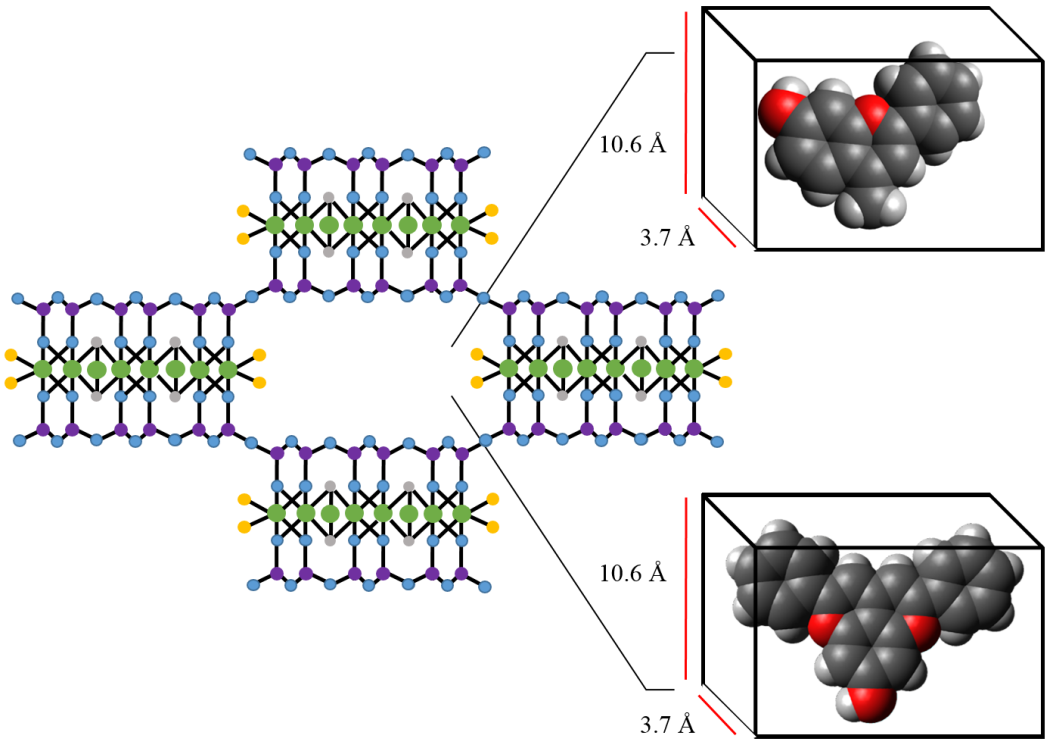


**Figure 1.** Comparison of the molecular sizes of FL3 (top) and PFL2 (bottom) with the dimensions of the tunnels of SEP.

The visible colors of some samples are more pronounced than those of others (Figure 2), a consequence of the relatively small quantities of FL and PFL cations adsorbed and differences in their molar absorptivities. More importantly, adsorption on the clays did have a significant effect on the chemical and thermal stability of the dyes, as well as the fluorescence efficiencies of several of them, as outlined in the following sections.

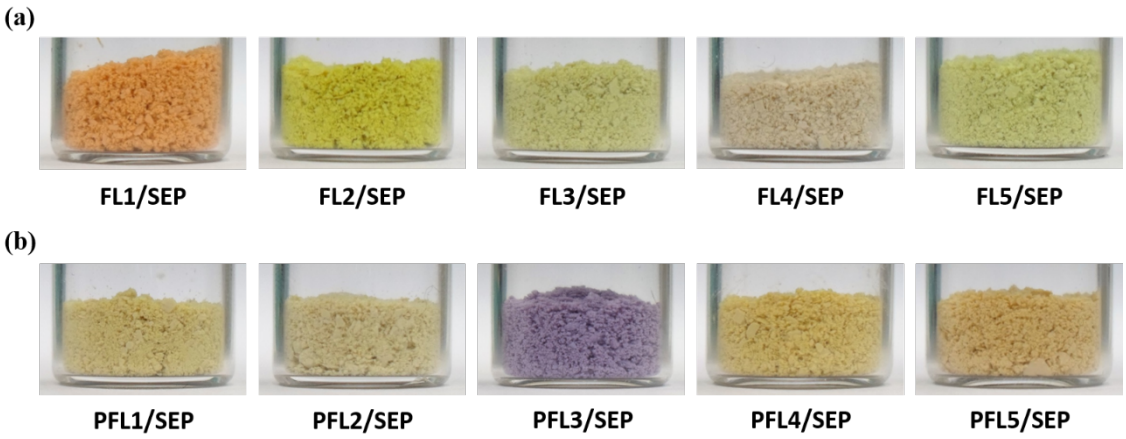


**Figure 2.** Images of the samples (a) FL/SEP and (b) PFL/SEP.

### 3.2 Chemical and thermal stability

For the thermal and chemical stability studies, the samples with most pronounced colors. i.e., FL1/SEP and PFL3/SEP (Figure 2) were chosen. The two classes of dyes studied here are largely unstable at high temperatures. Thus, while both FL1 and PFL3 degrade substantially in < 2 h at either 105 °C or 120 °C, FL1/SEP largely retained its characteristic colors for 24 h at both of these temperatures. At 105 ºC, PFL3/SEP still retained its characteristic color for 24 h, but at 120 °C major degradation occurred (Figure 3), with an accompanying obvious change in color (Figure 4).

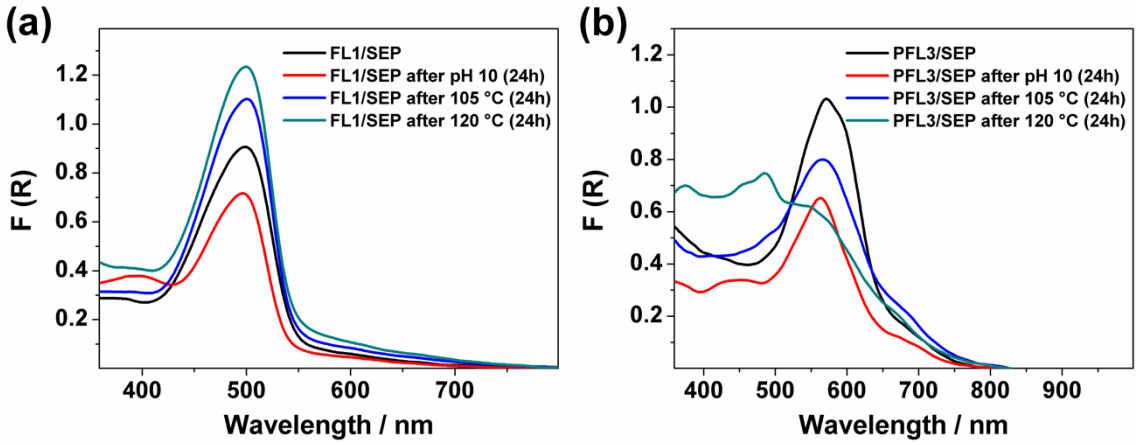


**Figure 3.** UV-Vis-DR spectra (Kubelka-Munk mode) of (a) FL1/SEP and (b) PFL3/SEP before and after immersion in pH 10 aqueous buffer.

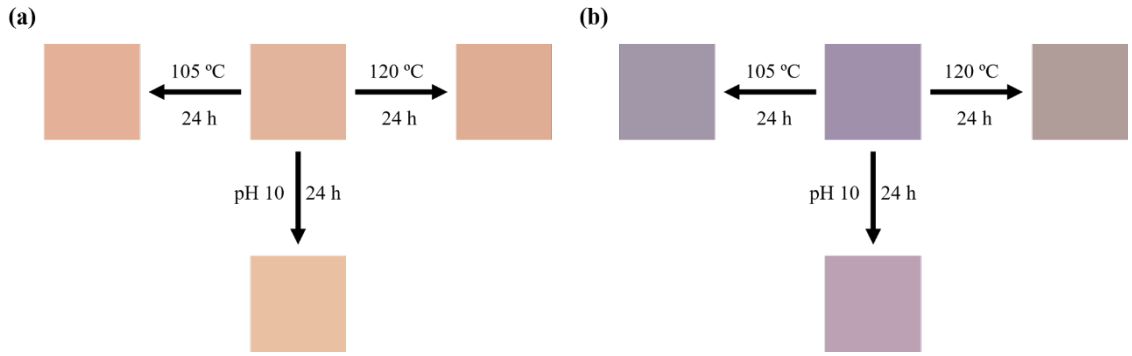


**Figure 4.** Images of the colors from CIELAB coordinate data for (a) FL1/SEP and (b) PFL3/SEP after the thermal stability tests.

In aqueous solution, FL1 begins to lose its color above about pH 3 ($pK_h$, or the pH at which half of the cation form is hydrated, is 3.0 ± 0.3)[47] due to the formation of the corresponding hemiacetal, followed by ring-opening tautomerization to form a cis-chalcone and then slow isomerization to the trans-chalcone.[47] PFL3 (like all of the PFLs used in this work) undergoes deprotonation of the 7-hydroxy group at basic pH[62] (see Figure S1 of the Supplementary Material). Figures 3 and 4 also show the impact on the spectra and colors of FL1/SEP and PFL3/SEP before and after immersion in a pH 10 aqueous buffer medium. The corresponding CIELAB color coordinates are listed in Table S1 of the Supplementary Material. Although the color of FL1/SEP became less intense, substantial color still remained, indicating that adsorbed FL1 is less prone to hydration. For PFL3/SEP, a new band appeared around 450 nm, similar to the band that appears for PFL3 in solution at high pH (Figure S2 of the Supplementary Material). However, the color of the sample only faded slightly and did not change abruptly as it does for PFL3 in solution (Figure S1 of the Supplementary Material). In neither case did the dye leach from the clay into the pH 10 aqueous medium.

The selective stabilization of the cationic form of FL1 by adsorption on SEP was further demonstrated by experiments in which FL1 was incubated with SEP in acetate

buffers at pH 4, 5 or 6. Prior to the addition of SEP (Figure 5a), the solution is nearly colorless due to the hydration reaction. Upon addition of SEP to these solutions, the suspended clay gradually acquired the orange color of the adsorbed FL1 cation as a function of time (Figure 5b). The rates of appearance of the coloration were qualitatively very similar at pH 4, 5 and 6 and the maximum intensity of the color was similar at all three pH values (Figure 5c). Because there are large pH-dependent differences in the equilibrium concentration of the cationic form in solution, this result strongly suggests that the hydrated forms of FL1 initially adsorb on SEP, where they subsequently convert to the cationic form by interaction with acidic sites of the SEP clay. Indeed, SEP clay has been reported to have two kinds of acid surface sites, one that is strongly acidic with an effective $pK_a$ around 3.2 - 3.3[59,63] and another that is moderately acidic with a $pK_a$ in the range of 6.3 – 6.6.[63,64]

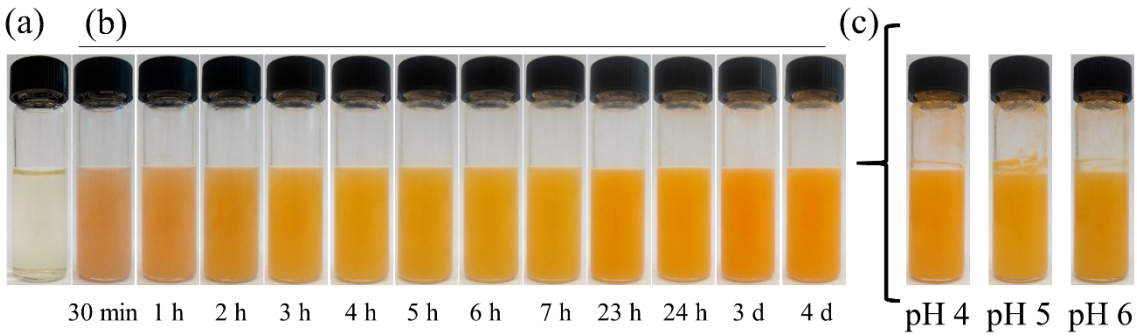


**Figure 5.** Images of (a) FL1 at pH 4; (b) mixture of FL1 and SEP as a function of time at pH 4; and (c) mixture of FL1 and SEP at pH 4, 5 and 6, after 27 days.

### 3.3. Spectroscopic studies

Figure 6 presents the UV-Vis-DR spectra for all of the hybrid pigments prepared in this work, plotted in the Kubelka-Munk mode as remission spectra (Eq. 1). All spectra had an underlying background absorption due to the SEP clay itself (the spectrum of SEP clay is shown in Figure S3 of the Supplementary Material). With the exception of FL4/SEP, PFL1/SEP and PFL2/SEP, the spectra are red shifted from those in acidic

solution (1 % 1.0 mol $dm^{-3}$ HCl/methanol for the FL cations[45] and acetonitrile containing 0.10 mol $dm^{-3}$ TFA for the PFL cations[65]), with the largest red shifts for FL1/SEP (ca. 22 nm), FL2/SEP (ca. 10 nm) and PFL3/SEP (ca. 20 nm). Red shifts of this type have been attributed to electrostatic interactions[66,67] or to the acidity of the inorganic substrate.[68] The exhaustive washing following the initial adsorption procedure was effective, eliminating any excess of FL and PFL cations since the spectra did not exhibit any evidence of the presence of aggregates of FL or PFL.

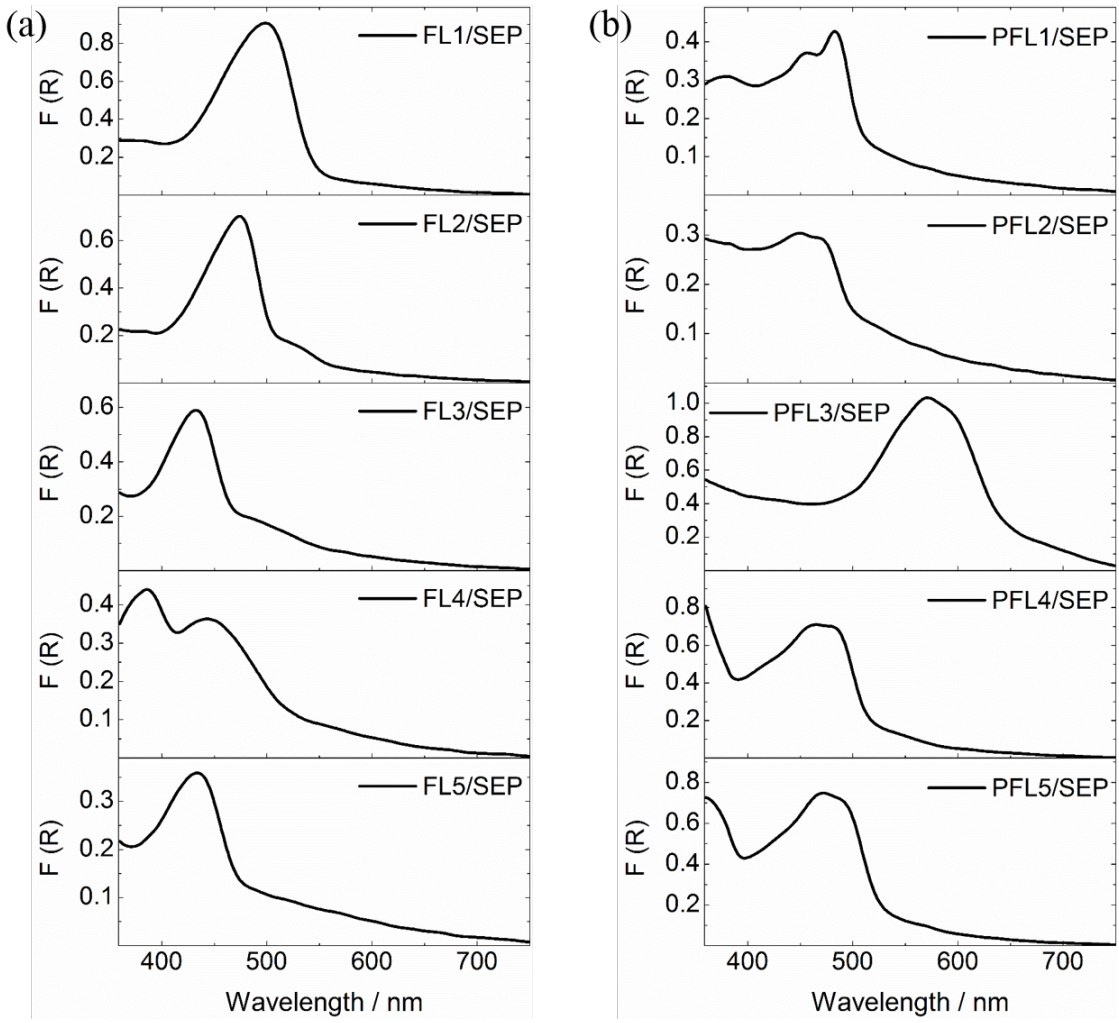


**Figure 6.** UV-Vis-DR spectra (Kubelka-Munk mode) of the (a) FL/SEP and (b) PFL/SEP samples.

Steady-state fluorescence excitation and emission spectra of the hybrid pigments are shown in Figure 7. The fluorescence excitation spectra for both classes of hybrid

pigments are generally similar to the remission spectra (Figure 6), with the exception of FL4/SEP whose emission was too weak to obtain a reliable spectrum. The fact that fluorescence could be observed at all from FL4/SEP and PFL3/SEP was an indication itself that the interaction with SEP improved the fluorescence of the dyes since both FL4 and PFL3 are essentially non-fluorescent in solution.

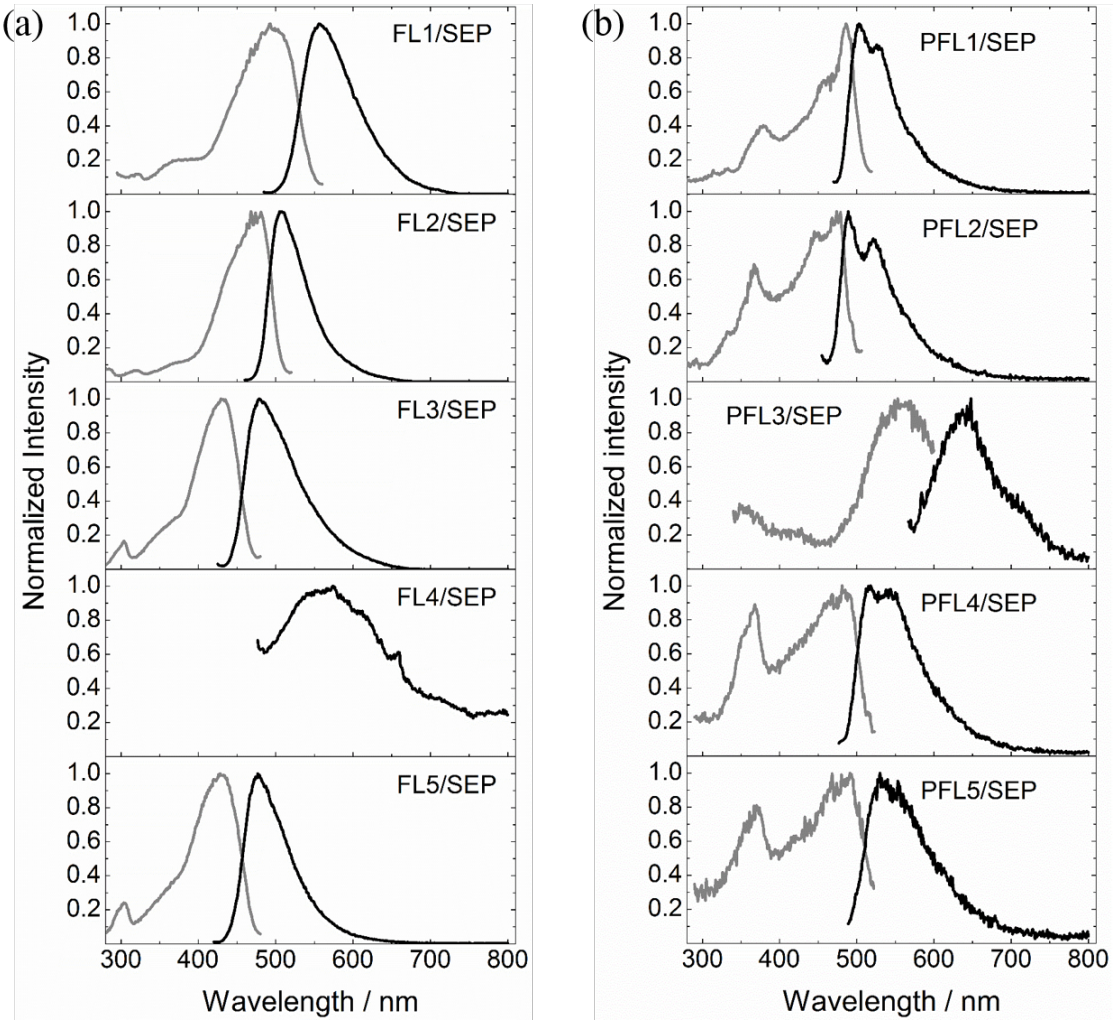


**Figure 7.** Excitation and emission spectra of the hybrid pigments (a) FL1/SEP (Ex. 480 and Em. 576 nm), FL2/SEP (Ex. 450 and Em. 530 nm), FL3/SEP (Ex. 415 and Em. 490 nm), FL4/SEP (Ex. 450), FL5/SEP (Ex. 410 and Em. 490 nm), and (b) PFL1/SEP (Ex. 455 and Em. 530 nm), PFL2/SEP (Ex. 445 and Em. 523 nm), PFL3/SEP (Ex. 555 and Em. 640 nm), PFL4/SEP (Ex. 450 and Em. 545 nm), PFL5/SEP (Ex. 455 and Em. 555 nm).

Figure 8 presents confocal fluorescence microscopic images (false-color mapping) of some of the more strongly fluorescent hybrid clay particles, pointing to relatively uniform emission across the whole particle. The impressive fluorescence of these solid samples instigated us to perform measurements of fluorescence quantum yields. The results, presented in Table 1, show that the fluorescence quantum yields of the FLs and PFLs tend to be equal to or slightly higher than those of the FLs and PFLs in acetonitrile containing 0.1 mol $dm^{-3}$ TFA. Particularly noteworthy are the large increase in the fluorescence quantum yield of FL1 in SEP and the observation of fluorescence from PFL3 in SEP. PFL3 is non-emissive in solution due to relaxation to a twisted intramolecular charge transfer (TICT) state[65] and encapsulation of FL1 in a CB[7] cucurbituril cavity was also found to strongly enhance its fluorescence.[47] Unlike FL5, which is quite fluorescent in solution, FL1 has an electron-rich dimethoxyphenyl B-ring that favors intramolecular charge-transfer interactions with the cationic portion of the molecule. Thus, adsorption of FL1 and PFL3 on sepiolite presumably inhibits the conformational changes in the excited singlet states that transform the fluorescent locally excited state into a much less fluorescent or non-fluorescent TICT state. The time-resolved emission decay measurements (Table 1) indicate two lifetime components that make roughly equal contributions to the emission. In the case of FL1 and FL2, the longer lifetime exceeds that of the dyes adsorbed on PAL (Table 1). Since no aggregates of FL or PFL cations were detected, the two lifetime components suggest the existence of at least two different adsorption sites, potentially reflecting binding of the dye in the external grooves and in the internal tunnels of SEP.

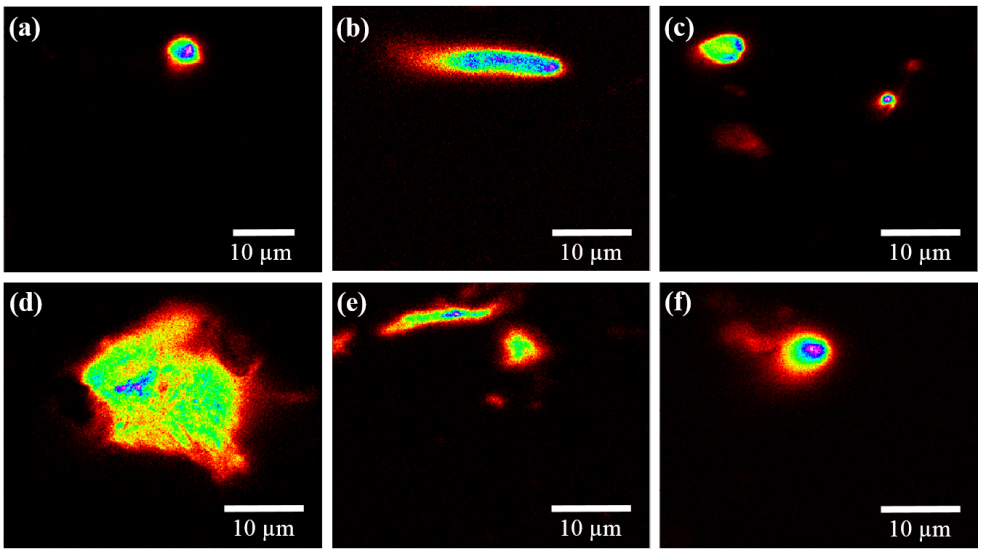


**Figure 8.** Confocal fluorescence images (false color) of the samples (a-b) FL2/SEP; (c) FL5/SEP; (d-e) PFL5/SEP and (f) PFL2/SEP.

**Table 1.** Quantum yields ($\Phi_f$) and lifetimes ($\tau_f$) for fluorescence of the FL and PFL cations adsorbed into/onto SEP.

| Hybrid pigments | $\Phi_f$* | $\Phi_f$[a] | $\tau_{f,1}$* / ns | $\tau_{f,2}$* / ns | $\tau_f$[b] / ns |
|---|---|---|---|---|---|
| **FL1/SEP** | 0.37 | 0.001 | 1.33 (41%) | 3.10 (59%) | 0.35 (80%)<br>1.0 (20%) |
| **FL2/SEP** | 0.41 | 0.42 | 1.11 (47%) | 2.95 (53%) | 0.6 (60%)<br>2.0 (40%) |
| **FL3/SEP** | 0.310 | 0.26 | 1.51 (52%) | 4.08 (48%) | |
| **FL4/SEP** | 0.006 | 0.001 | - | - | |
| **FL5/SEP** | 0.61 | 0.53 | 1.86 (33%) | 5.72 (67%) | |
| **PFL1/SEP** | 0.36 | 0.43[c] 0.41[d] | 0.83 (56%) | 3.61 (44%) | |
| **PFL2/SEP** | 0.22 | 0.16[c] | 2.13 (47%) | 6.48 (53%) | |

| | | | | |
|---|---|---|---|---|
| **PFL3/SEP** | 0.027 | - | - | - |
| **PFL4/SEP** | 0.067 | 0.048[c] | 1.36 (61%) | 3.96 (39%) |
| **PFL5/SEP** | 0.044 | 0.030[c] | 0.79 (74%) | 2.62 (26%) |

[*]±10 %; [a]FLs and PFLs at 20°C in air-equilibrated acetonitrile containing 0.10 mol $dm^{-3}$ TFA. [b]FLs adsorbed on PAL, Ref. [45]. [c]Ref. [69]. [d]Ref. [70].

## 4. Conclusions

The adsorption of flavylium (FL) and pyranoflavylium (PFL) cations on sepiolite (SEP) clay results in hybrid materials with a series of improved properties in terms of stability of the color in contact with mildly basic aqueous solution, resistance to thermal degradation of the dye, while maintaining excellent fluorescence properties. In all cases, the SEP-adsorbed dyes are at least as fluorescent as in solution, with particular attention to FL1, which is substantially more fluorescent. The thermal stability of FL1/SEP is better than that of PFL3/SEP, suggesting that the smaller FL1 dye molecules are perhaps more readily incorporated in the tunnels of SEP than the larger PFL3 dye molecules. FL1 is also more resistant to color loss due to hydration when adsorbed on SEP, with its wider tunnels and grooves, than on PAL clay[45] with narrower tunnels and grooves. The fluorescence decays of FL and PFL adsorbed on SEP are biexponential, with a somewhat greater contribution from the longer decay time for FL than for PFL, suggesting that the longer and shorter fluorescence lifetimes arise from dye adsorbed in the SEP tunnels and grooves, respectively. SEP thus appears to be a promising substrate for the development of highly fluorescent hybrid pigments with improved color and thermal stability.

## Acknowledgements

This study was financed in part by the Coordenação de Aperfeiçoamento de Pessoal de

Nível Superior - Brasil (CAPES) - Finance Code 001. The authors also thank the CNPq (F.H.Q. Universal grant 408181/2016-3), INCT-Catálise (CNPq 465454/2014-3), and NAP-PhotoTech for the support, the CNPq for a research productivity fellowships (F.H.Q. and M.H.G.) and undergraduate fellowship (K.M.S.), and CAPES for graduate fellowships (G.T.M.S. and C.P.S.). Researchers at UVic thanks NSERC (RGPIN-2017-04458) for funding and CAMTEC for the use of shared facilities. A.C.B.R. thanks the project no. 22124-LLPT-Laserlab-Portugal (ref: CENTRO-01-0145-FEDER-000014) for a post-doctoral grant.

## References


1 M. F. Brigatti, E. Galan and B. K. G. Theng, in *Chapter 2, Handbook of Clay Science, Developments in Clay Science*, 2006, vol. 1, pp. 19–86.

2 E. Galan, Properties and applications of palygorskite-sepiolite clays, *Clay Miner.*, 1996, **31**, 443–453.

3 V. Martínez-Martínez, C. Corcóstegui, J. Bañuelos Prieto, L. Gartzia, S. Salleres and I. López Arbeloa, Distribution and orientation study of dyes intercalated into single sepiolite fibers. A confocal fluorescence microscopy approach, *J. Mater. Chem.*, 2011, **21**, 269–276.

4 E. Ruiz-Hitzky, Molecular access to intracrystalline tunnels of sepiolite, *J. Mater. Chem.*, 2001, **11**, 86–91.

5 D. Karataş, A. Tekin and M. S. Çelik, Density functional theory computation of organic compound penetration into sepiolite tunnels, *Clays Clay Miner.*, 2017, **65**, 1–13.

6 S. Ovarlez, F. Giulieri, A. Chaze and F. Delamare, The Incorporation of Indigo Molecules in Sepiolite Tunnels, *Chem. - A Eur. J.*, 2009, **15**, 11326–11332.

7 M. Sánchez Del Río and P. Martinetto, Synthesis and Acid Resistance of Maya Blue Pigment, *Archaeometry*, 2006, **48**, 115–130.

8 E. Arnold and J. Branden, The first direct evidence for the production of Maya Blue: rediscovery of a technology, *Antiquity*, 2008, **82**, 151–164.

9 G. Chiari, R. Giustetto, J. Druzik, E. Doehne and G. Ricchiardi, Pre-columbian nanotechnology: Reconciling the mysteries of the maya blue pigment, *Appl. Phys. A Mater. Sci. Process.*, 2008, **90**, 3–7.

10 A. Tilocca and E. Fois, The color and stability of maya blue: TDDFT calculations, *J. Phys. Chem. C*, 2009, **113**, 8683–8687.

11 R. Giustetto, F. X. Llabrés I Xamena, G. Ricchiardi, S. Bordiga, A. Damin, R. Gobetto and M. R. Chierotti, Maya blue: A computational and spectroscopic study, *J. Phys. Chem. B*, 2005, **109**, 19360–19368.

12 R. Giustetto, D. Levy and G. Chiari, Crystal structure refinement of Maya Blue pigment prepared with deuterated indigo, using neutron powder diffraction, *Eur. J. Mineral.*, 2006, **18**, 629–640.

13 R. Giustetto, D. Levy, O. Wahyudi, G. Ricchiardi and J. G. Vitillo, Crystal structure refinement of a sepiolite/indigo Maya Blue pigment using molecular modelling and synchrotron diffraction, *Eur. J. Mineral.*, 2011, **23**, 449–466.

14 E. Lima, A. Guzmán, M. Vera, J. L. Rivera and J. Fraissard, Aged natural and synthetic Maya Blue-like pigments: What difference does it make?, *J. Phys. Chem. C*, 2012, **116**, 4556–4563.

15 R. Giustetto, K. Seenivasan, F. Bonino, G. Ricchiardi, S. Bordiga, M. R. Chierotti and R. Gobetto, Host/guest interactions in a sepiolite-based maya blue pigment: A spectroscopic study, *J. Phys. Chem. C*, 2011, **115**, 16764–16776.

16 A. Doménech, M. T. Doménech-Carbó and H. G. M. Edwards, On the interpretation of the Raman spectra of Maya Blue: A review on the literature data, *J. Raman Spectrosc.*, 2011, **42**, 86–96.

17 C. Tsiantos, M. Tsampodimou, G. H. Kacandes, M. Sánchez Del Río, V. Gionis and G. D. Chryssikos, Vibrational investigation of indigo-palygorskite association(s) in synthetic Maya blue, *J. Mater. Sci.*, 2012, **47**, 3415–3428.

18 A. Doménech-Carbó, M. T. Doménech-Carbó, F. M. Valle-Algarra, M. E. Domine and L. Osete-Cortina, On the dehydroindigo contribution to Maya Blue, *J. Mater. Sci.*, 2013, **48**, 7171–7183.

19 G. Chiari, R. Giustetto and G. Ricchiardi, Crystal structure refinements of

palygorskite and Maya Blue from molecular modelling and powder synchrotron diffraction, *Eur. J. Mineral.*, 2003, **15**, 21–33.

20 R. Giustetto, O. Wahyudi, I. Corazzari and F. Turci, Chemical stability and dehydration behavior of a sepiolite/indigo Maya Blue pigment, *Appl. Clay Sci.*, 2011, **52**, 41–50.

21 Y. Zhang, J. Dong, H. Sun, B. Yu, Z. Zhu, J. Zhang and A. Wang, Solvatochromic Coatings with Self-Cleaning Property from Palygorskite@Polysiloxane/Crystal Violet Lactone, *ACS Appl. Mater. Interfaces*, 2016, **8**, 27346–27352.

22 Y. Zhang, J. Zhang and A. Wang, From Maya blue to biomimetic pigments: durable biomimetic pigments with self-cleaning property, *J. Mater. Chem. A*, 2016, **4**, 901–907.

23 S. Wu, J. Huang, H. Cui, T. Ye, F. Hao, W. Xiong, P. Liu and H. Luo, Preparation of organic–inorganic hybrid methylene blue polymerized organosilane/sepiolite pigments with superhydrophobic and self-cleaning properties, *Text. Res. J.*, , DOI:10.1177/0040517519829924.

24 Y. Zhang, J. Zhang and A. Wang, Facile preparation of stable palygorskite/methyl violet@SiO2 “Maya Violet” pigment, *J. Colloid Interface Sci.*, 2015, **457**, 254–263.

25 L. Fan, Y. Zhang, J. Zhang and A. Wang, Facile preparation of stable palygorskite/cationic red X-GRL@SiO $_2$ “Maya Red” pigments, *RSC Adv.*, 2014, **4**, 63485–63493.

26 Y. Zhang, W. Wang, B. Mu, Q. Wang and A. Wang, Effect of grinding time on fabricating a stable methylene blue/palygorskite hybrid nanocomposite, *Powder Technol.*, 2015, **280**, 173–179.

27 Q. Wang, B. Mu, Y. Zhang, J. Zhang and A. Wang, Palygorskite-based hybrid

fluorescent pigment: Preparation, spectroscopic characterization and environmental stability, *Microporous Mesoporous Mater.*, 2016, **224**, 107–115.

28 Y. Zhang, L. Fan, H. Chen, J. Zhang, Y. Zhang and A. Wang, Learning from ancient Maya: Preparation of stable palygorskite/methylene blue@SiO2 Maya Blue-like pigment, *Microporous Mesoporous Mater.*, 2015, **211**, 124–133.

29 R. Giustetto, J. G. Vitillo, I. Corazzari and F. Turci, Evolution and reversibility of host/guest interactions with temperature changes in a methyl red@palygorskite polyfunctional hybrid nanocomposite, *J. Phys. Chem. C*, 2014, **118**, 19322–19337.

30 R. Giustetto and O. Wahyudi, Sorption of red dyes on palygorskite: Synthesis and stability of red/purple Mayan nanocomposites, *Microporous Mesoporous Mater.*, 2011, **142**, 221–235.

31 S. Wu, Z. Duan, F. Hao, S. Xiong, W. Xiong, Y. Lv, P. Liu and H. Luo, Preparation of acid-activated sepiolite/Rhodamine B@SiO2 hybrid fluorescent pigments with high stability, *Dye. Pigment.*, 2017, **137**, 395–402.

32 S. Wu, H. Cui, C. Wang, F. Hao, P. Liu and W. Xiong, In situ self-assembled preparation of the hybrid nanopigment from raw sepiolite with excellent stability and optical performance, *Appl. Clay Sci.*, 2018, **163**, 1–9.

33 G. Tian, W. Wang, D. Wang, Q. Wang and A. Wang, Novel environment friendly inorganic red pigments based on attapulgite, *Powder Technol.*, 2017, **315**, 60–67.

34 Q. Wang, B. Mu, W. Wang, A. Wang and G. Tian, Cost-efficient, vivid and stable red hybrid pigments derived from naturally available sepiolite and halloysite, *Ceram. Int.*, 2016, **43**, 1862–1869.

35 H. Li, A. Zhang, A. Wang, B. Mu and X. An, Cobalt blue hybrid pigment doped with magnesium derived from sepiolite, *Appl. Clay Sci.*, 2018, **157**, 111–120.

36 L. F. Casassa and J. F. Harbertson, Extraction, Evolution, and Sensory Impact of

Phenolic Compounds During Red Wine Maceration, *Annu. Rev. Food Sci. Technol.*, 2014, **5**, 83–109.

37 J. Heras-Roger, C. Díaz-Romero and J. Darias-Martín, What Gives a Wine Its Strong Red Color? Main Correlations Affecting Copigmentation, *J. Agric. Food Chem.*, 2016, **64**, 6567–6574.

38 K. Tang, T. Liu, Y. Han, Y. Xu and J. M. Li, The Importance of Monomeric Anthocyanins in the Definition of Wine Colour Properties, *South African J. Enol. Vitic.*, 2017, **38**, 1–10.

39 R. Brouillard, S. Chassaing and A. Fougerousse, Why are grape/fresh wine anthocyanins so simple and why is it that red wine color lasts so long?, *Phytochemistry*, 2003, **64**, 1179–1186.

40 M. Schwarz, T. C. Wabnitz and P. Winterhalter, Pathway Leading to the Formation of Anthocyanin−Vinylphenol Adducts and Related Pigments in Red Wines, *J. Agric. Food Chem.*, 2003, **51**, 3682–3687.

41 H. Fulcrand, M. Dueñas, E. Salas and V. Cheynier, Phenolic reactions during winemaking and aging, *Am. J. Enol. Vitic.*, 2006, **57**, 289–297.

42 A. Marquez, M. P. Serratosa and J. Merida, Pyranoanthocyanin Derived Pigments in Wine: Structure and Formation during Winemaking, *J. Chem.*, 2013, **2013**, 1–15.

43 J. Oliveira, N. Mateus and V. de Freitas, Previous and recent advances in pyranoanthocyanins equilibria in aqueous solution, *Dye. Pigment.*, 2014, **100**, 190–200.

44 M. Figueiredo-González, B. Cancho-Grande, J. Simal-Gándara, N. Teixeira, N. Mateus and V. De Freitas, The phenolic chemistry and spectrochemistry of red sweet wine-making and oak-aging, *Food Chem.*, 2014, **152**, 522–530.

45 G. T. M. Silva, C. P. Silva, M. H. Gehlen, J. Oake, C. Bohne and F. H. Quina, Organic/inorganic hybrid pigments from flavylium cations and palygorskite, *Appl. Clay Sci.*, 2018, **162**, 478–486.

46 A. A. Freitas, A. A. L. Maçanita and F. H. Quina, Improved analysis of excited state proton transfer kinetics by the combination of standard and convolution methods., *Photochem. Photobiol. Sci.*, 2013, **12**, 902–10.

47 B. Held, H. Tang, P. Natarajan, C. P. Silva, V. O. Silva, C. Bohne and F. H. Quina, Cucurbit[7]uril inclusion complexation as a supramolecular strategy for color stabilization of anthocyanin model compounds, *Photochem. Photobiol. Sci.*, 2016, **15**, 752–757.

48 C. P. Silva, R. M. Pioli, L. Liu, S. Zheng, M. Zhang, G. T. M. Silva, V. M. T. Carneiro and F. H. Quina, Improved Synthesis of Analogues of Red Wine Pyranoanthocyanin Pigments, *ACS Omega*, 2018, **3**, 954–960.

49 J. Madejová, W. P. Gates and S. Petit, in *Chapter 5, Handbook of Clay Science, Developments in Clay Science*, 2017, vol. 8, pp. 107–149.

50 C. He, E. Makovicky and B. Osbæck, Thermal treatment and pozzolanic activity of sepiolite, *Appl. Clay Sci.*, 1996, **10**, 337–349.

51 M. K. Wang, P. C. Tseng, S. S. Chang, D. T. Ray, Y. H. Shau, Y. W. Shen, R. C. Chen and P. N. Chiang, Origin and mineralogy of sepiolite and palygorskite from the tuluanshan formation, eastern taiwan, *Clays Clay Miner.*, 2009, **57**, 521–530.

52 V. Gionis, G. H. Kacandes, I. D. Kastritis and G. D. Chryssikos, Combined near-infrared and x-ray diffraction investigation of the octahedral sheet composition of palygorskite, *Clays Clay Miner.*, 2007, **55**, 543–553.

53 C. Vogt, J. Lauterjung and R. X. Fischer, Investigation of the Clay Fraction (<2 μm ) of the Clay Minerals Society Reference Clays, *Clays Clay Miner.*, 2002, **50**,

388–400.

54 M. R. Weir, W. Kuang, G. A. Facey and C. Detellier, Solid-state nuclear magnetic resonance study of sepiolite and partially dehydrated sepiolite, *Clays Clay Miner.*, 2002, **50**, 240–247.

55 B. Hubbard, W. Kuang, A. Moser, G. A. Facey and C. Detellier, Structural study of Maya Blue: Textural, thermal and solid-state multinuclear magnetic resonance characterization of the palygorskite-indigo and sepiolite-indigo adducts, *Clays Clay Miner.*, 2003, **51**, 318–326.

56 Z. Li, C. A. Willms and K. Kniola, Removal of anionic contaminants using surfactant-modified palygorskite and sepiolite, *Clays Clay Miner.*, 2003, **51**, 445–451.

57 A. Gilchrist and J. Nobbs, *Encycl. Spectrosc. Spectrom. Second Ed.*, 1999, 380–385.

58 E. P. Tomasini, E. S. Román and S. E. Braslavsky, Validation of fluorescence quantum yields for light-scattering powdered samples by laser-induced optoacoustic spectroscopy, *Langmuir*, 2009, **25**, 5861–5868.

59 S. Tunç, O. Duman and R. Uysal, Electrokinetic and Rheological Behaviors of Sepiolite Suspensions in the Presence of Poly(acrylic acid sodium salt)s, Polyacrylamides, and Poly(ethylene glycol)s of Different Molecular Weights, *J. Appl. Polym. Sci.*, 2008, **109**, 1850–1860.

60 H. Shariatmadari, A. R. Mermut and M. B. Benke, Sorption of selected cationic and neutral organic molecules on palygorskite and sepiolite, *Clays Clay Miner.*, 1999, **47**, 44–53.

61 F. L. Arbeloa, T. L. Arbeloa and I. L. Arbeloa, Spectroscopy of Rhodamine 6G Adsorbed on Sepiolite Aqueous Suspensions, *J. Colloid Interface Sci.*, 2002, **187**,

105–112.

62 A. A. Freitas, C. P. Silva, G. T. M. Silva, A. L. Maçanita and F. H. Quina, Ground- and Excited-State Acidity of Analogs of Red Wine Pyranoanthocyanins, *Photochem. Photobiol.*, 2018, **94**, 1086–1091.

63 M. S. Çelik, in *Clay Surfaces: Fundamentals and Applications*, 2004, vol. 1, pp. 57–89.

64 M. Alkan, Ö. Demirbaş and M. Doğan, Electrokinetic properties of sepiolite suspensions in different electrolyte media, *J. Colloid Interface Sci.*, 2005, **281**, 240–248.

65 F. Siddique, C. P. Silva, G. T. M. Silva, H. Lischka, F. H. Quina and A. J. A. Aquino, The electronic transitions of analogs of red wine pyranoanthocyanin pigments, *Photochem. Photobiol. Sci.*, 2019, **18**, 45–53.

66 Y. Kohno, Y. Shibata, N. Oyaizu, K. Yoda, M. Shibata and R. Matsushima, Stabilization of flavylium dye by incorporation into the pore of protonated zeolites, *Microporous Mesoporous Mater.*, 2008, **114**, 373–379.

67 Y. Kohno, R. Kinoshita, S. Ikoma, K. Yoda, M. Shibata, R. Matsushima, Y. Tomita, Y. Maeda and K. Kobayashi, Stabilization of natural anthocyanin by intercalation into montmorillonite, *Appl. Clay Sci.*, 2009, **42**, 519–523.

68 Y. Kohno, S. Tsubota, Y. Shibata, K. Nozawa, K. Yoda, M. Shibata and R. Matsushima, Enhancement of the photostability of flavylium dye adsorbed on mesoporous silicate, *Microporous Mesoporous Mater.*, 2008, **116**, 70–76.

69 G. T. M. Silva, S. S. Thomas, C. P. Silva, J. C. Schlothauer, M. S. Baptista, A. A. Freitas, C. Bohne and F. H. Quina, Triplet Excited States and Singlet Oxygen Production by Analogs of Red Wine Pyranoanthocyanins, *Photochem. Photobiol.*, 2018, **95**, 176–182.

70 A. A. Freitas, C. P. Silva, G. T. M. Silva, A. L. Maçanita and F. H. Quina, From vine to wine: photophysics of a pyranoflavylium analog of red wine pyranoanthocyanins, *Pure Appl. Chem.*, 2017, **89**, 1761–1767.